PFC/JA-82-8

QUASILINEAR THEORY CALCULATION OF ION TAILS AND NEUTRON RATES DURING LOWER HYBRID HEATING IN ALCATOR A

J. J. Schuss, T. M. Antonsen, Jr., M. Porkolab

Plasma Fusion Center
Massachusetts Institute of Technology
Cambridge, MA 02139

May 1982

This work was supported by the U.S. Department of Energy Contract No. DE-AC02-78ET51013. Reproduction, translation, publication, use and disposal, in whole or in part by or for the United States government is permitted.

QUASILINEAR THEORY CALCULATION OF ION TAILS AND NEUTRON RATES DURING LOWER HYBRID HEATING IN ALCATOR A

J. J. Schuss, T. M. Antonsen Jr.*, M. Porkolab
Plasma Fusion Center
Massachusetts Institute of Technology
Cambridge, MA 02139

ABSTRACT

The steady state fast ion distribution function and the resulting neutron rate are calculated for the conditions of the Alcator A lower hybrid heating experiment from quasilinear theory. First, ion orbit losses are ignored and the steady state ion distribution function is calculated. It is found that in this case the experimental neutron rates and neutron rate decay times are consistent with only a small fraction of the incident RF power being absorbed in the plasma center. This absorbed power is centered in the regime $3.5 < n_{\|} < 4.5$. A Monte Carlo ion simulation technique, which incorporates ripple orbit losses is then presented that calculates the steady state ion distribution function in the presence of the RF. The results of this simulation require approximately 50% of the incident RF power to be dissipated in the plasma core in order to obtain agreement with the experimental results. Most of this RF power is lost to ripple trapped ions. These calculations demonstrate the importance of orbit losses in determining lower hybrid heating efficiencies and additionally provide a technique for calculating them.

* Present address: Department of Physics and Astronomy, University of Maryland, College Park, Maryland 20742.

I. Introduction

Lower hybrid heating experiments have been carried out in a number of tokamaks. In several of these experiments the RF has been observed to produce energetic ion tails.[1—6] In the case of the Alcator A lower hybrid heating experiment[4—6] a factor of 50 enhancement to the thermal neutron rate was produced when the RF was applied. This neutron production was due to an energetic ion tail produced by the RF wave at the plasma center. From the neutron rate decay time τ_N which was longer than 1.5 msec, it was deduced that this ion tail had a temperature $T_T > 15$ keV and extended to an energy $E_{max} > 50$ keV. In Ref. 6 it was shown that these minimum values for T_T and E_{max} were required by the slowing down of the tail ions on electrons. For a machine such as Alcator A, energetic ion orbit losses almost certainly affect this energetic ion distribution function. Since in the ion heating mode the RF first deposits its energy into this energetic ion tail, the absence of perfect ion confinement will reduce the fraction of tail ion power deposited into the bulk plasma and therefore lower bulk plasma RF heating efficiencies.

Karney[7,8] has shown that above an RF power threshold the ion motion, under the influence of the lower hybrid wave, becomes stochastic. When this threshold is far exceeded, perpendicular unmagnetized ion Landau damping can be recovered.[9] This treatment then obtains a velocity space diffusion coefficient which can be used to calculate the ion distribution function. This threshold is[7,8]

$$\frac{E_o}{B_o} > \frac{1}{4}\left(\frac{\omega_{ci}}{\omega}\right)^{1/3}\frac{\omega}{k_\perp c} \tag{1}$$

Here $\vec{k} = (k_\perp, k_\parallel)$, where $\vec{k}\cdot\vec{B}_o/|\vec{B}_o| = k_\parallel$ and $|\vec{k}\times\vec{B}_o|/|\vec{B}_o| = k_\perp$. $k_\perp$ is determined by the dispersion relation

$$k_\perp^4\epsilon_{xx2} + k_\perp^2\epsilon_{xx0} + k_\parallel^2\epsilon_{zz0} = 0 \tag{2}$$

where

$$\epsilon_{xx0} = 1 + \frac{\omega_{pe}^2}{\omega_{ce}^2} - \frac{\omega_{pi}^2}{\omega^2}$$

$$\epsilon_{zz0} = 1 - \frac{\omega_{pe}^2}{\omega^2}$$

$$\epsilon_{xx2} = -\frac{3}{4}\frac{T_e}{m_e\omega_{ce}^2}\frac{\omega_{pe}^2}{\omega_{ce}^2} - 3\frac{\omega_{pi}^2}{\omega^2}\frac{T_i}{m_i\omega^2}$$

and E_o can be determined by the RF power flux per unit area

$$S = \frac{E_o^2\omega\left(\epsilon_{xx0} + 2\epsilon_{xx2}k_\perp^2\right)}{8\pi k_\perp} \tag{3}$$

For the case of Alcator A ($n_e \sim 2 \times 10^{14}$, $T_e = 900$ eV, $T_i = 800$ eV, $B_o = 62$ kG, deuterium, $R = 54$ cm, $r_L = 10$ cm, $P_{RF} = 70$ kW and a waveguide area $= 20$ cm^2) and for $k_{\|} = 5\omega/c$, we have $k_\perp = 157$/cm and $E_o \simeq 25$ kV/cm. This far exceeds the threshold field of Eq. (1) of $E_o \simeq 4$ kV/cm. However, this estimate assumes that the RF power propagates into the plasma core as a well defined lower hybrid resonance cone. During the Alcator A experiment CO_2 laser scattering indicated that the RF waves in the plasma interior approximately uniformly filled the plasma cross section and did not exhibit well defined cones.[10] In this case in determining the field E_o we must take the external area of the plasma core $A = 2\pi R 2\pi \Delta r$ (here as an example we take $\Delta r = 3$ cm) in determining S and E_o. This obtains $E_o \approx 2$ kV/cm, which is less than the field of Eq. (1). The threshold given by Eq. (1) applies to the case in which the confining magnetic field is uniform and the RF energy is in a single monochromatic wave. In the case of practical interest where the magnetic field is nonuniform and the RF energy consists of a spectrum of waves the threshold may be lower than given by Eq. (1).

In the remainder of this paper we shall assume the validity of quasilinear theory and employ diffusion coefficients similar to those of Karney.[9] Quasilinear theory has already been applied to the Wega experiment and was not found to be inconsistent.[10] Here we shall first assume perfect ion confinement and calculate ion tails and bulk heating in Section II. It will be shown that in this case the neutron rates of the Alcator A experiment can be produced by a small amount of RF power. In Section III a Monte Carlo technique will be introduced from which ion distribution functions and power balance can be calculated. In Section IV this technique will be applied to the Alcator A experiment using a heuristic ripple loss model. There it is found that most of the applied RF power is lost to ripple-trapped ions and not deposited into the bulk plasma. Finally, in Section V the results are summarized.

II. Fast Ion Calculation in the Absence of Orbit Losses

Here we assume that there are no orbit losses and calculate the local $f_i(\vec{v})$ in the presence of the lower hybrid wave. We assume that the ions are unmagnetized and use the quasilinear diffusion coefficient for unmagnetized ions[12]

$$\overline{\overline{D}}(\vec{v}) = 8\pi^2 \frac{e^2}{m^2} \int_{-\infty}^{\infty} dk_\perp \epsilon_{k_\perp} \frac{\vec{k}\vec{k}}{k^2} \delta(\vec{k} \cdot \vec{v} - \omega) \tag{4}$$

where

$$\epsilon_{k_\perp} = \frac{1}{16\pi^2 L} \left| \hat{E}(k_\perp) \right|^2$$

$$\hat{E}(k_\perp) = \int_{-\infty}^{\infty} dx e^{-ik_\perp x} \hat{E}(x)$$

where we are considering a one dimensional variation in $\tilde{E}(\tilde{x})$ along the direction of $\vec{k}(k_\perp \gg k_\parallel)$. We note that we can express $\epsilon_{k_\perp}$ as

$$8\pi^2\epsilon_{k_\perp} = \frac{\pi}{2}E_o^2\frac{G(k_\perp)}{\Delta} \tag{5}$$

where

$$\int_{-\infty}^{\infty} dk_\perp G(k_\perp) = \Delta \equiv k_{\perp max} - k_{\perp min}$$

($G(k_\perp)$ is just a form factor for $|\tilde{E}(k_\perp)|^2$). We let the $k_\perp$ spectrum extend from $k_{\perp min}$ to $k_{\perp max}$. (The remaining expressions are now of the same form as in Ref. 9.) Since $f_o(\tilde{v}) = f_o(v_\parallel, v_\perp)$ and there is no zero order dependence on the cyclotron orbit angle, we can average Eq. (4) (as done in Ref. 9).

$$\begin{aligned} D(v_\perp) &= \frac{1}{2\pi}\int_0^{2\pi} d\psi \frac{\pi}{2}\frac{e^2E_o^2}{m^2}\int dk_\perp \frac{G(k_\perp)}{\Delta}\cos^2\psi\delta(\omega - k_\perp v_\perp\cos\psi) \\ &= \frac{1}{2}\frac{e^2E_o^2}{m^2}\frac{\omega^2}{v_\perp^2}\int_{-\infty}^{\infty}\frac{dk_\perp}{\Delta}\frac{G(k_\perp)}{k_\perp^2(k_\perp^2v_\perp^2 - \omega^2)^{1/2}} \end{aligned} \tag{6}$$

Then we obtain the diffusion equation

$$\begin{aligned} \frac{\partial f_o(v_\perp)}{\partial t} &= \frac{1}{v_\perp\partial v_\perp}(v_\perp D(v_\perp))\frac{\partial f}{\partial v_\perp} \\ &\quad + \left(\frac{\partial f}{\partial t}\right)_{\text{collisions}} \end{aligned} \tag{7}$$

This equation has been solved in steady state assuming $F_o(\tilde{v}) = (m_i/2\pi T_i)^{1/2}\exp(-\frac{1}{2}m_iv_\parallel^2/T_i)F(v_\perp)$.

The solution of Eq. (7) is[9]

$$F(v_\perp) = F_o\exp\left[-\int_0^{v_\perp}\frac{v_\perp/v_{ti}^2 dv_\perp}{1 + D(v_\perp)/C(v_\perp)}\right],$$

where

$$\begin{aligned} C(v_\perp) &= \frac{6\pi n_e e^4\ln\Lambda}{m_i^{3/2}T^{3/2}}\left(\frac{v_{ti}^3}{v_\perp^3} + \frac{v_{ti}^3}{v_o^3}\right), \\ \frac{v_o^3}{v_{ti}^3} &= \frac{9Z_i}{2(2/\pi)^{1/2}}\left(\frac{m_i}{m_e}\right)^{1/2}, \end{aligned} \tag{8}$$

$v_{ti}^2 = T/m_i, T_e = T_i = T$, and $F(v_\perp)$ is the steady state perpendicular ion distribution function. For deuterium $v_o = 7.0v_{ti}$. The power dissipated by the wave is[9]

$$P_d = \frac{2\pi n_e m_i^2}{T}\int_0^{\infty}\frac{dv_\perp F(v_\perp)D(v_\perp)v_\perp^3}{1 + D(v_\perp)/C(v_\perp)} \tag{9}$$

The D-D neutron rate resulting from this tail is

$$R_N = n_e^2 \int_0^\infty 2\pi v_\perp dv_\perp \sigma(v_\perp) v_\perp F(v_\perp) \tag{10}$$

where $\sigma(v_\perp)$ is the neutron rate production cross section as a function of relative ion velocity. From Eq. (10) we can calculate the rate of decay of R_N at the time the RF is turned off

$$\frac{dR_N}{dt} = n_e^2 \int_0^\infty 2\pi v_\perp dv_\perp \sigma(v_\perp) v_\perp \frac{dF(v_\perp)}{dt} \tag{11}$$

Integrating by parts, using Eq. (7) and noting that $\partial F/\partial v_\perp|_\infty = \partial F/\partial v_\perp|_o = 0$, we obtain

$$\frac{dR_N}{dt} = n_e^2 \int_0^\infty \frac{m_i v_\perp^2}{T_i} \frac{D(v_\perp)C(v_\perp)}{D(v_\perp)+C(v_\perp)} F(v_\perp) \frac{\partial}{\partial v_\perp}(v_\perp \sigma(v_\perp)) 2\pi dv_\perp \tag{12}$$

from which we can define a neutron rate decay time $\tau_N = R_N/|dR_N/dt|$. We note that in order to properly normalize $F(v_\perp)$ we let $F_o = m_i/(2\pi T_i)\delta'$, $\delta' \sim 1$, and is selected to normalize $\int F(v_\perp) 2\pi dv_\perp = 1$. The power flux incident on the plasma can be calculated from Eq. (3).

In doing these calculations, we need to select a well behaved $G(k_\perp)$. If we let $G(k_\perp) = \Delta\delta(k_\perp - k_{\perp o})$, the resulting diffusion coefficient has a singularity at $\omega/k_{\perp o}$, which will complicate these one dimensional calculations and make impossible the Monte Carlo code to be presented in the following sections. This diffusion coefficient is graphed as $D_o(v_\perp)$ in Fig. 1. If we choose $G(k_\perp)$ to be a parabolic function of $k_\perp$, i.e.

$$G(k_\perp) = \frac{6}{\Delta^2}(k_{\perp max} - k_\perp)(k_\perp - k_{\perp min}) \tag{13}$$

then the resulting $D(v_\perp)$ and its derivative $D'(v_\perp)$ are well behaved and are simple algebraic functions; these are graphed in Fig. 1 as $D_1(v_\perp)$ and $D_1'(v_\perp)$. In the remainder of this paper the $G(k_\perp)$ of Eq. (13) will be used in $D(v_\perp)$.

Figure 2 shows $F(v_\perp)$ vs. $E_\perp$ for three different values of electric field E_o. We see that ion tails extending out to tens of keV's can be present for values of E_o comparable to those of the Alcator A experiment. If we use Eq. (12) to calculate τ_N, we find that the highest value of $E = 2500$ V/cm results in a $\tau_N = 1.7$ msec, which is consistent with the experimental value of $\tau_N \gtrsim 1.5$ msec.[6] However, the lowest value of $E = 700$ V/cm results in a $\tau_N = 0.83$ msec, which is clearly inconsistent with the experimental observations. From this we see that only suprathermal ion tails similar to those of $E = 2500$ V/cm can be consistent with the experiment.

In Fig. 3a we apply this calculation to the case of Alcator A ($n_e = 2.4 \times 10^{14}$ cm^{-3}, $T_i = T = 800$ eV, $B_T = 6.2$ T, deuterium). Here we plot the ratio between the thermal neutron rate and the RF tail produced

neutron rate (i.e., the neutron rate enhancement) and the power dissipated in W/cm^3. We assume values of E_o which are consistent with the indicated RF power being uniformly incident on the plasma core having $r = \Delta r < 3$ cm (the limiter radius is $r = 10$ cm). In the absence of RF most of the thermally produced neutrons originate from $r < 3$ cm. In Fig. 3 it is assumed that $k_{zmin} = 3.5\omega/c$ and $k_{zmax} = 4.5\omega/c$, from which $k_{\perp max}$ and $k_{\perp min}$ are calculated through Eq. (2) by letting $k_{\parallel} = k_{zmax}$ and k_{zmin}, respectively. A factor of 50 enhancement in the neutron rate corresponds to an incident RF power of 46 kW and to $E_o = 1640$ V/cm. This also corresponds to $P_d = 0.33$ W/cm^3, which for a plasma core volume of 9.6×10^3 cm^3 yields a total RF power dissipation of 3.2 kW. Figure 3b plots τ_N vs. incident power; for this value of E_o we have $\tau_N \approx 1.5$ msec. These results are consistent with the Alcator A experiment.

In Fig. 4a we plot the neutron rate enhancement and the power dissipation for the same parameters as those of Fig. 3 except that here $k_{zmax} = 5\omega/c$ and $k_{zmin} = 4\omega/c$. In Fig. 4a we see that the damping is much stronger as evidenced by an order of magnitude higher dissipation per unit volume. A factor of 50 enhancement in the neutron rate corresponds to an incident power less than 20 kW or $E_o < 1237$ V/cm. However, this results in $\tau_N < 1.1$ msec (from Fig. 4b), which is not consistent with the experimental neutron rate decay time. Values of k_{zmax}, k_{zmin} lower than 3.5 – 4.5 result in damping rates and neutron production rates that are too small to produce observable plasma effects.

In summary, the preceding calculations show that if ion orbit losses were absent only a small fraction ($<$ 10%) of the net incident RF power of 75 kW was actually dissipated in the central plasma core in Alcator A during ion heating. However, the ion tails calculated extend past $E_\perp = 50$ keV, where it is well known that extreme orbit losses exist. In the following sections this problem will be addressed.

III. Monte Carlo Simulation Method

In the preceding section we considered an approximate solution of the Fokker Planck equation. The solution was obtained by balancing the various terms describing the diffusion and slowing down of a particle's perpendicular velocity. The effects of pitch angle scattering and the details of the dependence of the distribution function on parallel velocity were ignored.

In a toroidal confinement device with significant ripple in the magnetic field, ions with sufficiently low parallel velocity can become trapped in a ripple well. If the trapped ion has sufficiently high energy it can then drift out of the device before colliding and becoming detrapped. This process will have the effect of removing at a very rapid rate those ions that occupy a region of velocity space corresponding to high energy and small

parallel velocity. Furthermore, this is precisely the region into which particles are scattered by the lower hybrid wave fields. Thus, it is necessary to solve the Fokker Planck equation in two dimensions in velocity space, $v_\perp$ and $v_\parallel$, and to include the effects of ripple losses and pitch angle scattering. To do this we have developed a Monte Carlo simulation code.

We wish to solve the Fokker-Planck equation in the presence of both collisions and RF induced quasilinear diffusion in $v_\perp$. This equation is

$$\frac{\partial f}{\partial t} = C(f) + Q(f) \tag{14}$$

where

$$\begin{aligned} Q(f) &= \frac{\partial}{\partial x}(4xD(x))\frac{\partial}{\partial x}f(x) \\ C(f) &= \frac{1}{2v^2}\frac{\partial}{\partial v}\left[v^2 < (\Delta v_\parallel)^2 > \frac{\partial f}{\partial v}\right] \\ &\quad + \frac{1}{4v^2}\frac{\partial}{\partial \xi}(1-\xi^2)\frac{\partial}{\partial \xi}(< (\Delta v_\perp)^2 > f) \\ &\quad - \frac{1}{v^2}\frac{\partial}{\partial v}\left[v^2\left(\frac{1}{2} < \Delta v_\parallel >_i + < \Delta v_\parallel >_e\right)f\right] \end{aligned}$$

where $x = v_\perp^2$ and $\xi = \vec{v}\cdot\vec{B}/(|\vec{v}\parallel\vec{B}|)$. $Q(f)$ is obtained from Eq. (7) by the change of variables. Here $\parallel$ refers to the direction parallel to the initial velocity before collision and $\perp$ is perpendicular to the initial velocity. $C(f)$ is due to collisions[9,13]; the collisional diffusion coefficients are[14]

$$\begin{aligned} \frac{1}{2} < \Delta v_\parallel >_i + < \Delta v_\parallel >_e &= -C\left[\frac{m_i}{2T_i}G(\ell_i v) + \frac{m_i}{2T_e}G(\ell_e v)\right] \\ < (\Delta v_\parallel)^2 > &= \frac{C}{v}[G(\ell_i v) + G(\ell_e v)] \\ < (\Delta v_\perp)^2 > &= \frac{C}{v}[\Phi(\ell_i v) - G(\ell_i v) \\ &\quad + \Phi(\ell_e v) - G(\ell_e v)] \end{aligned} \tag{15}$$

$$C = \frac{8\pi n_e e^4 \ln\Lambda}{m_i^2} \qquad \ell_i = \sqrt{\frac{m_i}{2T_i}} \qquad \ell_e = \sqrt{\frac{m_e}{2T_e}}$$

$$G(x) = [\Phi(x) - x\Phi'(x)]/2x^2 \qquad \Phi(x) = \frac{2}{\sqrt{\pi}}\int_0^x e^{-y^2}dy$$

We shall use the expressions of Eq. (15) for both $\ell_i v \gg 1$ and $\ell_i v \ll 1$ in the calculations and therefore require

a simple analytical approximation to the Coulomb diffusion coefficients. We shall use those of Ref. 15, namely

$$G(x) \approx \frac{\rho x}{1+2\rho x^3},$$

$$\Phi(x) \approx \frac{\rho(3x+2x^3)}{1+2\rho x^3}, \qquad \rho = \frac{2}{3\sqrt{\pi}}. \tag{16}$$

Since the ion orbits can be complex, we shall solve Eq. (14) by using a Monte Carlo technique. In the resulting code, the ion is allowed to move a small distance along its orbit. At the endpoint of this segment, the ion undergoes a random scattering event; the time Δt of this segment is kept short so that changes in $\vec{v}$ are small compared to the initial velocity components. In this sequence the ion is first scattered in ξ, then in $|v|$ (and slowed down appropriately), and then scattered in $v_\perp$ due to the RF quasilinear operator. In the RF scattering the diffusion coefficient of Eq. (6) is employed with the $G(k_\perp)$ of Eq. (13). The scattering technique is that of Ref. 9. The ion takes a step in x

$$\Delta x = \begin{cases} \delta^+ & \text{probability } \frac{1}{2} \\ -\delta^- & \text{probability } \frac{1}{2} \end{cases} \tag{17}$$

Here we let

$$\delta^+(x) = \sqrt{2(4xD(x))\Delta t}, \tag{18}$$

and $\delta^-(x)$ is chosen by the relation

$$\delta^-(x+2\delta(x)) = \delta(x). \tag{19}$$

Equation (19) properly takes into account the derivatives of $D(x)$ and satisfies the requirement that an initially flat $f(x)$ remain so under diffusion. In addition, it does not permit ions to diffuse below $v_\perp = \omega/k_{\perp max}$ due to the RF fields. A Taylor expansion of Eq. (19) yields

$$\delta^+(x) - \delta^-(x) \approx \frac{d\delta^2(x)}{dx} \tag{20}$$

We then see, as expected, that this prescription is equivalent to

$$\sigma^2 = 2(4xD(x))\Delta t$$

$$< x > = x + \Delta t \frac{d}{dx}(4xD(x)) \tag{21}$$

where now $4xD(x)$ is the diffusion coefficient. Figure 5 shows a typical graph of $\delta^+(x)$ and $\delta^-(x)$ for parameters similar to those of Alcator A and for $\Delta t = 0.1$ μsec. The offset of $\delta^-(x)$ from $\delta^+(x)$ is due to Eq. (19). We note that for $v_\perp < \omega/k_{\perp max}$, $\delta^+(x) = \delta^-(x) = 0$ and there is no quasilinear scattering.

The Coulomb scattering of ξ is treated in the manner of Ref. 16. At the end of the time step Δt, a new ξ is chosen from a Gaussian probability distribution function, i.e.,

$$P(\xi) = \frac{1}{\sqrt{2\pi}\sigma} \exp\left[-\frac{(\xi - \xi_m)^2}{2\sigma^2}\right] \tag{22}$$

where

$$\sigma_\xi^2 = 2D_\xi \Delta t$$

$$\xi_m = = < \xi > = \xi_o + \Delta t \frac{dD_\xi}{d\xi}|_{\xi_o}$$

$$D_\xi = \frac{1-\xi^2}{4v^2} < (\Delta v_\perp)^2 >$$

and ξ_o is the value of ξ before scattering. By calculating $\frac{d<v>}{dt}$ and $\frac{d<v^2>}{dt}$ the scattering in $|\vec{v}| = v$ can be obtained using a method similar to that of Ref. 17. We obtain

$$\sigma_v^2 = 2D_v \Delta t$$

$$v_m = = < v > = v_o + \Delta t \frac{dD_v}{dv} + \Delta t \left(\frac{2D_v}{v} + \frac{1}{2} < \Delta v_\parallel >_i + < \Delta v_\parallel >_e \right)$$

$$D_v = \frac{1}{2} < (\Delta v_\parallel)^2 > \tag{23}$$

The last term in v_m is the Coulomb term that corresponds to ion slowing. In the simulations presented below it was found that this prescription produced the proper Maxwellian distribution function for $v_\perp < \omega/k_{\perp max}$. For example, when the dD_v/dv term was removed from the expression for v_m, the distribution function no longer was Maxwellian for $v \sim \sqrt{2T_i/m_i}$.

Finally, we need a prescription for finding the steady state distribution function $f_{ss}(\vec{v})$. It satisfies the equation

$$\frac{\partial f_{ss}}{\partial t} = 0 = C(f_{ss}) + Q(f_{ss}) + S(\vec{v}) \tag{24}$$

where $S(\vec{v})$ represents a source of ions at $v \lesssim v_{ti}$. Here we are treating the case where there is a loss region in velocity space and a source is required for a steady state solution. The Monte Carlo code solves for $g(\vec{v}, t)$ where

$$\frac{\partial g}{\partial t} = C(g) + Q(g) \tag{25}$$

If we integrate Eq. (25) from $t = 0$ to $t = \infty$ we obtain

∂t (25)

If we integrate Eq. (25) from $t = 0$ to $t = \infty$ we obtain

$$\int_0^\infty \frac{\partial g}{\partial t} dt = g(\infty) - g(0)$$

$$= \int_0^\infty dt[C(g) + Q(g)]$$

$$= C\left(\int_0^\infty g dt\right) + Q\left(\int_0^\infty g dt\right). \tag{26}$$

If $g(\infty) = 0$ (i.e., we integrate in time numerically until all ions are lost) we see that

$$f_{ss}(\vec{v}) = A \int_0^\infty g(\vec{v}) dt, \tag{27a}$$

and

$$Ag(0) = S(\vec{v}). \tag{27b}$$

The quantity A is a normalization constant. Similarly, it can be shown that

$$\int d^3v \frac{1}{2} m v^2 C(f_{ss}) = A \int_0^\infty dt \int d^3v \frac{1}{2} m v^2 C(g)$$

$$= \text{steady state collisional power to bulk plasma} = P_{PL}, \tag{28}$$

and

$$\int d^3v \frac{1}{2} m v^2 Q(f_{ss}) = A \int_0^\infty dt \int d^3v \frac{1}{2} m v^2 Q(g)$$

$$= \text{steady state rf dissipation} = P_{RF},$$

or that the steady state power flows are equal to the time integrals of the power flows of the Monte Carlo solution. From this prescription we can obtain the steady state f_{ss} and power balance from the simulation. In calculating the heating efficiency, we must take into account the energy of the ion source term; i.e., $P_{TH} = Ag(o)\frac{1}{2} m v_1^2$, where v_1 is the initial ion energy. The RF heating efficiency is then $EFF = [(P_{PL} - P_{TH})_{RF\,ON} - (P_{PL} - P_{TH})_{RF\,OFF}]/P_{RF}$. The P_{TH} term can be made arbitrarily small by reducing $\frac{1}{2} m v_1^2$.

IV. Simulation of Alcator A Lower Hybrid Heating

We shall apply the method of Section III to calculate ion orbit losses in the Alcator A experiment.[6] It has been shown that ions in Alcator A are subject to ripple trapping losses due to the ripple $\delta = \Delta B/B = 2\%$ on axis.[18] (Here $\Delta B = B_{max} - B_{min}, B =< B >$). These ripple losses cause the ripple trapped ions within the magnetic well (those having $v_\parallel/v = \xi < \delta^{1/2}$) to be depleted at energies above E_ℓ, where[18]

$$E_\ell = \left[\frac{8\pi}{2^{7/2}} \frac{n_i e^4 \ln \Lambda m_i^{1/2} a R \omega_{ci}}{\delta}\right]^{2/5} \tag{29}$$

This loss then produces an effective hole in velocity space which is illustrated in Fig. 6. The effect of this loss process will be treated in a manner similar to that of Ref. 19, where ion losses were calculated without RF using a heuristic ripple loss model. The ion will circumnavigate the torus at $r = 0$. The magnetic field on axis is modeled in each of the four wells as

$$B_T(\phi) = \begin{cases} B_o & |\phi| > \frac{\pi}{4N} \\ B_o(1-\delta) & |\phi| < \frac{\pi}{4N} \end{cases} \tag{30}$$

Here $N = 5$ and ϕ is the toroidal angle. $\phi = 0$ corresponds to the center of the ripple well. Equation (30) is true for $|\phi| < \frac{\pi}{4}$; it is repeated every 90° centered at each of the four ripple wells. During this orbit the ion is forced to scatter due to collisions and due to the RF several times both within and outside the ripple well. If the ion finds itself having $\xi < \delta^{1/2}$ while it is within the magnetic well, it is treated as being immediately ripple lost. This simplified orbit model neglects the effect of banana orbits; however, it is much faster to execute on a computer than a full orbit model and should allow an estimate of the effect of orbit losses on the fast ions. Furthermore, it will serve to demonstrate the technique of Section III. These simulations will be done using Alcator A parameters ($n_e = 2.4 \times 10^{14}$ cm^{-3}, $T_e = 1$ keV, $T_i = 800$ eV, deuterium, $B_T = 62$ kG, and $f = 2.45$ GHz). $E_o, k_{\perp max}$, and $k_{\perp min}$ will be varied.

Figure 7 shows the results of following 1000 deuterium ions for 333 μsec under the influence of the RF. Each ion starts off having $E = 5$ keV and $\xi = 0.1$. Here $E_o = 2.5$ kV/cm, $k_{\perp max} = 233$/cm, and $k_{\perp min} = 150$/cm. In this example we do not try to determine $f_{ss}(\tilde{v})$ by the procedure of Section III, but only study the time evolution of these ions due to the wave. At energies $E \gg T_i$, collisional slowing will dominate energy diffusion; therefore, in this example, if $E < \frac{1}{2} m_i(\omega/k_{\perp max})^2$ and if $E < E_\ell$, it is unlikely the ion will be ripple lost or RF scattered in times short compared to an energy diffusion time. We then count its energy as being deposited or "dumped" into the bulk plasma. Figure 7a shows the number of ions remaining orbiting the torus N_2 that have not been dumped or ripple lost as a function of time. N_1 is the number of ions not ripple

lost. Figure 7b shows the time evolution of the energy lost to the ripple, E_{RIP}, the RF energy, E_{RF}, the energy deposited by collisions into the plasma, E_{PL}, and the energy of the dumped ions, E_D. $E_{RIP} > E_{RF}$ here, as some of the initial thermal energy of the ions is lost when they scatter into the ripple well. When this simulation is carried out with $E_o = 0$, after 333 μsec it is found that 91% of the initial ion energy is deposited into the plasma, with 6% ripple lost (3% remains in ions orbiting the torus). With $E_o = 2.5$ kV/cm, at the end of 333 μsec the plasma absorbs an energy equal to 38% of the initial thermal energy; the RF has deposited an energy equal to 123% of the initial thermal energy into these ions and an energy equal to 31% of the initial thermal energy remains in ions orbiting the torus. We thus see that at least for this class of ions and for $t < 333\mu$sec the plasma actually cools when the RF is applied. Figure 7c shows the distribution of fast ions at $t = 33\mu$sec, 165 μsec and 333 μsec. In a time less than 1 msec the ions are kicked up to energies $E > 40$ keV.

While the previous calculation illustrates the effect of the RF on the fast ions, it does not predict the steady state power balance or $f_{ss}(\hat{v})$. This will now be presented using the prescription of Section III. Each ion is started with $E < T_i$ and is allowed to diffuse due to collisions or due to the RF until it is lost. Then $\int_0^\infty g(\hat{v}, t)dt$ is calculated and properly normalized. The normalization constant allows a calculation of the steady state power balance through Eq. (28). In addition, this code will calculate ΔN_i where

$$\Delta N_i \simeq F(E)\Delta E \tag{31}$$

and is the fraction of ions in steady state located at $E_i - \Delta E/2 < E < E_i + \Delta E/2$. The neutron rate in steady state is then ($n_i = n_e$)

$$R_N = n_e^2 \sum_i \Delta N_i \sigma(E_i)(2E_i/m_i)^{1/2} \tag{32}$$

and the decay rate of R_N after RF shutoff is

$$\frac{dR_N}{dt} = n_e^2 \sum_i \Delta N_i \frac{d}{dE_i}\left[\sigma(E_i)(2E_i/m_i)^{1/2}\right]\frac{dE_i}{dt} \tag{33}$$

where[16]

$$\frac{dE_i}{dt} = -\frac{2}{\tau_s}\frac{E_i^{3/2} + E_c^{3/2}}{E_i^{1/2}} \tag{34}$$

Equation (34) represents fast ions slowing on ions and electrons; $\tau_s = (3/8)(2/\pi)^{1/2} m_i T_e^{3/2}/(m_e^{1/2} n_e e^4 \ln\Lambda)$ and $E_c = 18.6T_e$. τ_N, the neutron rate decay time, is then $R_N/(dR_N/dt)$ and can be compared with the experimental time of $\gtrsim 1.5$ msec. It should be noted that the decay time of Eq. (33) may overestimate the neutron rate decay time, as it does not include ion orbit losses after RF turnoff.

Figures 8a and 8b show the distribution function of fast deuterium ions in steady state for $E_o = 2$ kV/cm, $k_{\perp max} = 220$ /cm and $k_{\perp min} = 165$ /cm; this corresponds to $k_{zmax} = 5.5\omega/c$ and $k_{zmin} = 4.5\omega/c$. Figure 8a shows that the calculated $f(v)$ is close to a Maxwellian for $E < 8$ keV. Above $E = 8$ keV the distribution function is essentially flat as in the calculation of Section II. Figure 8b shows the distribution function over a larger range in E. The RF produced tail extends to $E > 70$ keV; this tail produces a neutron rate enhancement over thermal of 111 and a decay time $\tau_N = 1.7$ msec. The RF power is $P_{RF} = 4.1$ W/cm^3, the power dumped into the ripple well $P_{RIP} = 5.25$ W/cm^3, the power deposited into the plasma $P_{PL} = -0.88$ W/cm^3, and the thermal source power $P_{TH} = +0.321$ W/cm^3. These RF values correspond to 37 kW of power incident on the $r = 3$ cm surface, all of which would be absorbed at this damping level. Figure 8c shows the distribution function $f(v)$ found by carrying out this simulation for $E_o = 0$. Due to the ripple losses there is substantial depletion above $E = 10$ keV. Here it is found that $P_{PL} = -1.14$ W/cm^3, $P_{RIP} = 1.34$ W/cm^3, and $P_{TH} = 0.197$ W/cm^3. Comparing the RF to the no RF case, according to the prescription of Section III, we find a bulk plasma heating efficiency of 3%. The remainder of the RF power is lost to the ripple well.

This previous simulation used 69 ions, yet due to the time averages the resulting distribution functions were well behaved. However, small statistical errors in the simulation that produce small ion tail changes also cause large changes in R_N as R_N is highly sensitive to ions having $E > 50$ keV. Keeping this in mind, Fig. 8 is consistent with the Alcator A RF ion heating results in both R_N and τ_N and indicates that most of the RF power is lost to the ripple well. It requires $P_{RF} > 30$ kW to reproduce the RF heating results, which is much more than the $P_{RF} < 5$ kW required when orbit losses are not included. Furthermore when we use values of $k_{zmax} = 5\omega/c, k_{zmin} = 4\omega/c$, the RF dissipation drops by 2 orders of magnitude and is too weak to have any effect. Thus the introduction of ion orbit losses requires an upshifting of the range of k_z's in the RF power spectrum of Section II.

V. Summary

In summary, we have used quasilinear theory to calculate the RF produced ion tails and neutron rates in the Alcator A experiment. If we ignore ion ripple losses, we find that the experimental results are consistent with the calculations if only several kilowatts of RF power having a power spectrum centered about $k_z = 4\omega/c$ are absorbed in the plasma center. However, the RF produced ion tail extends to $E > 50$ keV, where orbit losses should be substantial. When these orbit losses are taken into account the simulation is consistent with the experiment when of the order of 30–40 kW of RF power is absorbed in the plasma core; this RF power is centered about $k_z = 5\omega/c$. Most of this RF power is lost to ripple trapped ions and is not deposited into the

bulk plasma. This latter result is consistent with previous conclusions, which inferred that a substantial fraction of the RF power was upshifted to $k_z = 5\omega/c$.[4-6] This latter result also requires substantial penetration of the waveguide launched RF power to the plasma core.

As previously noted, while the distribution functions produced by the simulation are reasonably well behaved and tend to converge as the number of ions is increased, the neutron rates are less accurate and are highly sensitive to small fluctuations in $f(E)$ at high E. To a lesser extent, the RF power deposited in the plasma is sensitive to the tail distribution function. This can be seen from Eq. (9) for $D(v_\perp)/C(v_\perp) \gg 1$

$$P_d = \frac{2\pi n_e m_i}{T} \int_{\omega/k_{\perp max}}^{\infty} dv_\perp F(v_\perp) C_o v_{ti}^3 \left(1 + \frac{v_\perp^3}{v_o^3}\right) \tag{35}$$

where $C_o = 6\pi n_e e^4 \ln\Lambda/(m_i^{3/2}T^{1/2})$. Finally, the lost ripple power is determined by the energy of the ion at the time it is lost in the code; P_{RIP} thus requires a large number of ions to achieve good convergence. These statistical errors can be minimized by using a large number of ions. Another possible method would be that of splitting and Russian roulette,[20] which would increase the number of ions being followed at high energies without disturbing the randomness of the code. This splitting technique could be employed in more sophisticated orbit codes in order to minimize execution time.

In conclusion, these results have indicated that the ion heating results of the Alcator A lower hybrid heating experiment were profoundly affected by ion orbit losses. More importantly, these results illustrate a method by which these orbit losses can be calculated for lower hybrid heating experiments.

Acknowledgements

The authors are happy to acknowledge valuable discussions with Dave Schissel concerning this work.

This work was supported by the U.S. Department of Energy Contract No. DE-AC02-78ET 51013.

References

1. S. Bernabei, C. Daughney, W. Hooke, et al in *Plasma Heating in Toroidal Devices*, (Proc. 3rd Symp. Varenna, 1974) (E. Sindoni, Ed.), Editrice Compositori, Bologna (1976) 68.

2. T. Nagashima, H. Fujisawa in *Heating in Toroidal Plasma* (Proc. Joint Varenna-Grenoble Int. Symp., Grenoble 1978) (T. Consoli, P. Caldirola, Eds.) Vol. 2, Pergamon, Elmsford, New York (1979) 281.

3. C. Gormezano, P. Blanc, M. Durvaux, et al, Proc. 3rd Topical Conf. on RF Plasma Heating, Pasadena (1978) paper A3.

4. J. J. Schuss, S. Fairfax, B. Kusse, R. R. Parker, M. Porkolab, D. Gwinn, I. Hutchinson, E. S. Marmar, D. Overskei, D. Pappas, L. S. Scaturro and S. Wolfe, Phys. Rev. Lett. 43, 274 (1979).

5. J. J. Schuss, M. Porkolab and Y. Takase, Bull. Am. Phys. Soc. 24, 1020 (1979).

6. J. J. Schuss, M. Porkolab, Y. Takase, D. Cope, S. Fairfax, M. Greenwald, D. Gwinn, I. H. Hutchinson, B. Kusse, E. Marmar, D. Overskei, D. Pappas, R. R. Parker, L. Scaturro, J. West and S. Wolfe, Nucl. Fusion 21, 427 (1981)

7. C. F. F. Karney and A. Bers Phys. Rev. Lett. 39, 550 (1977).

8. C. F. F. Karney, Phys. Fluids 21, 1584 (1978).

9. C. F. F. Karney, Phys. Fluids 22, 2188 (1979).

10. C. M. Surko, R. E. Slusher, J. J. Schuss et al, Phys. Rev. Lett. 43, 1016 (1979).

11. C. Gormezano, W. Hess, G. Ichtchenko, et al, Nucl. Fusion 21, 1047 (1981).

12. Ira B. Bernstein and Folker Engelmann, Phys. Fluids 9, 937 (1966).

13. B.A. Trubnikov, in Review of Plasma Physics, edited by M.A. Leontovich (Consultants Bureau, New York, 1965), Vol. 1, p. 105.

14. L. Spitzer Jr., *The Physics of Fully Ionized Gases*, 2nd Revised Edition, Interscience, New York (1962).

15. T. H. Stix, Nucl. Fusion 15, 737 (1975).

16. R. J. Goldston, *Fast Ion Diagnostic Experiment on ATC: Radially Resolved Measurements of* q, Z_{eff}, $T_{i\|}$ *and* $T_{i\perp}$ PhD Thesis, Princeton University (1977).

17. Allen H. Boozer and Gioietta Kuo-Petravic, Phys. Fluids 24, 851 (1981).

18. M. Greenwald, J. J. Schuss, D. Cope, Nucl. Fusion 20, 783 (1980).

19. J. J. Schuss, Nucl. Fusion 20, 1160 (1980).

20. M. H. Hughes and D. E. Post, Journal of Computational Physics 28, 43 (1978).

Figure Captions

Fig. 1. RF diffusion coefficients D_o, D_1, and $D_1' = dD_1/dv$, where D_o is composed by letting $G(k_\perp) = \Delta\delta(k_\perp - k_{\perp o})$ and where D_1 is composed by letting $G(k_\perp) = (6/\Delta^2)(k_{\perp max} - k_\perp)(k_\perp - k_{\perp min})$. For D_o, $k_{\perp o} = 192$ /cm and for D_1, $k_{\perp max} = 233$ /cm, $k_{\perp min} = 150$ /cm.

Fig. 2. Graph of $F(E_\perp)$ vs. $E_\perp$ for 3 values of E_o and the conditions of the Alcator A experiment ($f = 2.45$GHz, $n_e = 2.4 \times 10^{14}$, $B_T = 62$kG, $T_e = 0.8$keV), and $n_{zmax} = 5$, $n_{zmin} = 4 (n_z = k_z c/\omega)$.

Fig. 3. (a) Graph of the neutron rate enhancement over thermal and the RF power dissipated vs. RF power incident on the plasma surface having $r = 3$ cm. Here $k_{zmax} = 4.5\omega/c$ and $k_{zmin} = 3.5\omega/c$, $n_e = 2.4 \times 10^{14}\text{cm}^{-3}$, $B_T = 62$kG, $T_e = T_i = 800$ eV and $f = 2.45$ GHz. (b) Neutron rate vs. incident RF power for the same conditions as in (a).

Fig. 4. (a) Graph of the neutron rate enhancement over thermal and the RF power dissipated vs. RF power incident on the plasma surface having $r = 3$ cm. Here $k_{zmax} = 5.0\omega/c$ and $k_{zmin} = 4\omega/c$, $n_e = 2.4 \times 10^{14}\text{cm}^{-3}$, $B_T = 62$kG, $T_e = T_i = 800$ eV and $f = 2.45$ GHz. (b) Neutron rate vs. incident RF power for the same conditions as in (a).

Fig. 5. Step sizes δ^+ and δ^- vs. $E_\perp$ from Eqs. (18-19) for $\Delta t = 0.1\mu$sec, $E_o = 2.5$ kV/cm, $k_{\perp max} = 233$/cm, $k_{\perp min} = 150$ /cm.

Fig. 6. Schematic of velocity space boundaries within the ripple well in Alcator A. The shaded region is the ripple loss region.

Fig. 7. Time evolution of simulation of 1000 ions under RF influence in Alcator A; $n_e = 2.4 \times 10^{14}\text{cm}^{-3}$, $B_T = 62$kG, $T_e = 1$ keV, $T_i = 800$ eV, $E_o = 2.5$ kV/cm, $k_{\perp max} = 233$/cm, $k_{\perp min} = 150$/cm, $k_{zmax} = 5.7\omega/c$ and $k_{zmin} = 4.2\omega/c$. (a) $N_1(t)$ and $N_2(t)$ vs. time. (b) Time evolution of E_{RIP}, E_{RF}, E_D, and E_p. (c) Fast ion distribution function for $t = 33\mu$sec, 165μsec, and 333μsec. The test ions have initial energy $E = 5$ keV and initial $\xi = 0.1$.

Fig. 8. Steady state distribution functions for $E_o = 2$ kV/cm, $k_{\perp max} = 220$ /cm, $k_{\perp min} = 165$ /cm, $k_{zmax} = 5.5\omega/c$, $k_{zmin} = 4.5\omega/c$, $n_e = 2.4 \times 10^{14}$, $B_T = 62$kG, $T_e = 1$keV, and $T_i = 800$ eV. (a) RF on; • = Maxwellian distribution. (b) same as (a) except that now E extends to 100 keV. (c) Same as (a) except now $E_o = 0$.

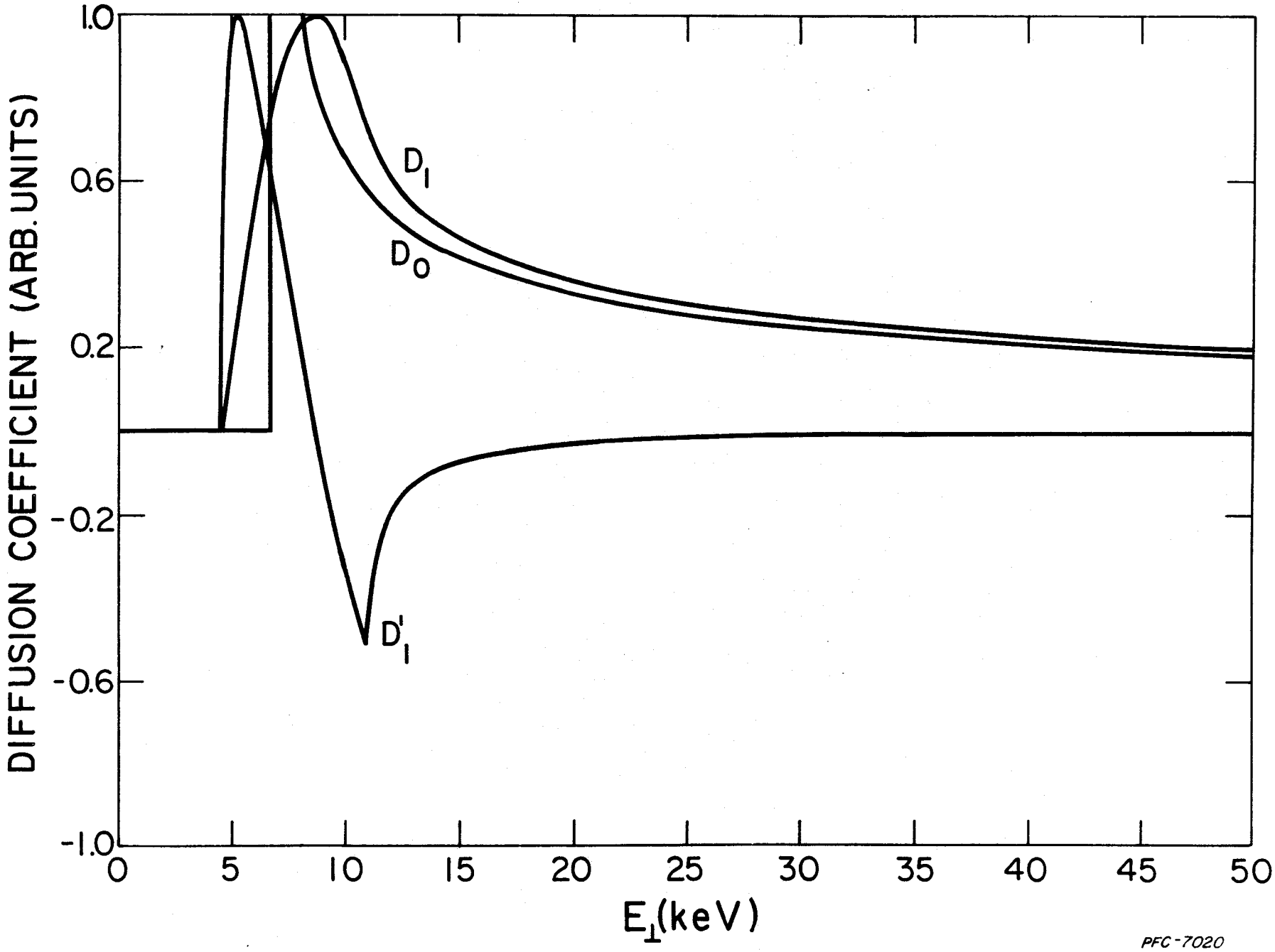
DIFFUSION COEFFICIENT (ARB. UNITS)
1.0
0.6
0.2
-0.2
-0.6
-1.0
0
5
10
15
20
25
30
35
40
45
50
$E_\perp$(keV)
D_1
D_0
D'_1
PFC-7020

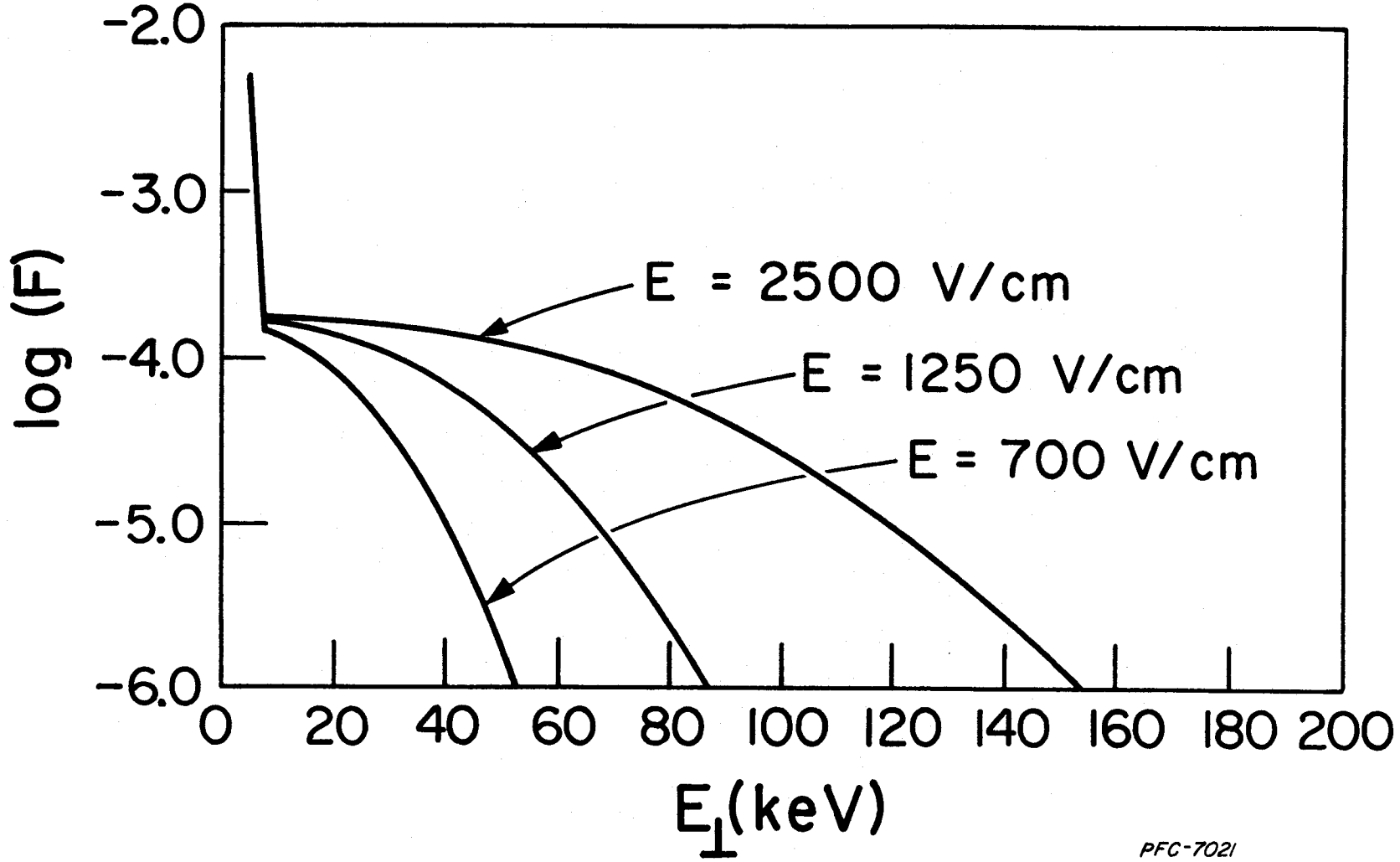
-2.0
-3.0
-4.0
-5.0
-6.0
log (F)
E = 2500 V/cm
E = 1250 V/cm
E = 700 V/cm
0
20
40
60
80
100
120
140
160
180
200
E⊥(keV)
PFC-7021

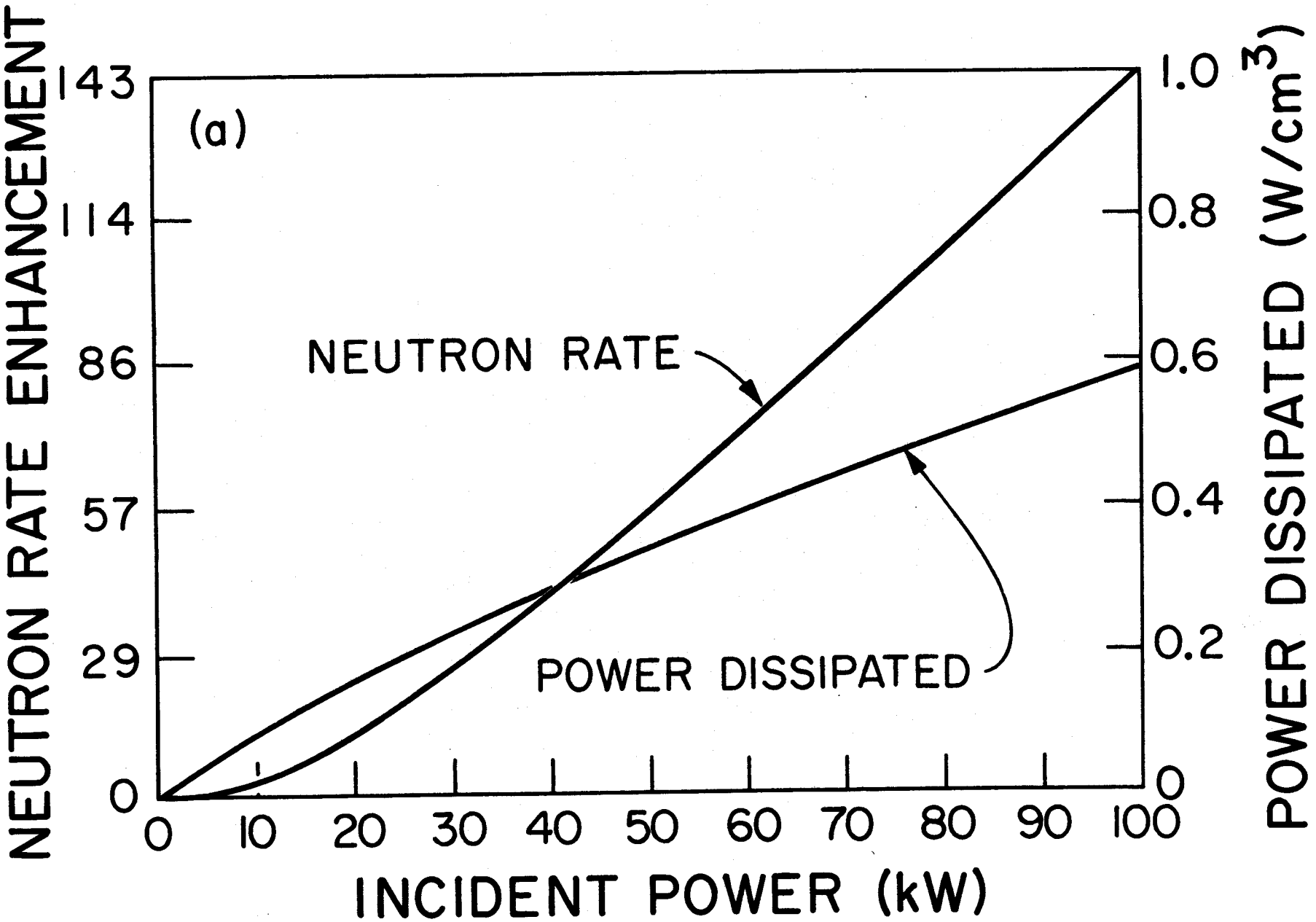
(a)
NEUTRON RATE ENHANCEMENT
143
114
86
57
29
0
NEUTRON RATE
POWER DISSIPATED
1.0
0.8
0.6
0.4
0.2
0
POWER DISSIPATED (W/cm3)
0 10 20 30 40 50 60 70 80 90 100
INCIDENT POWER (kW)

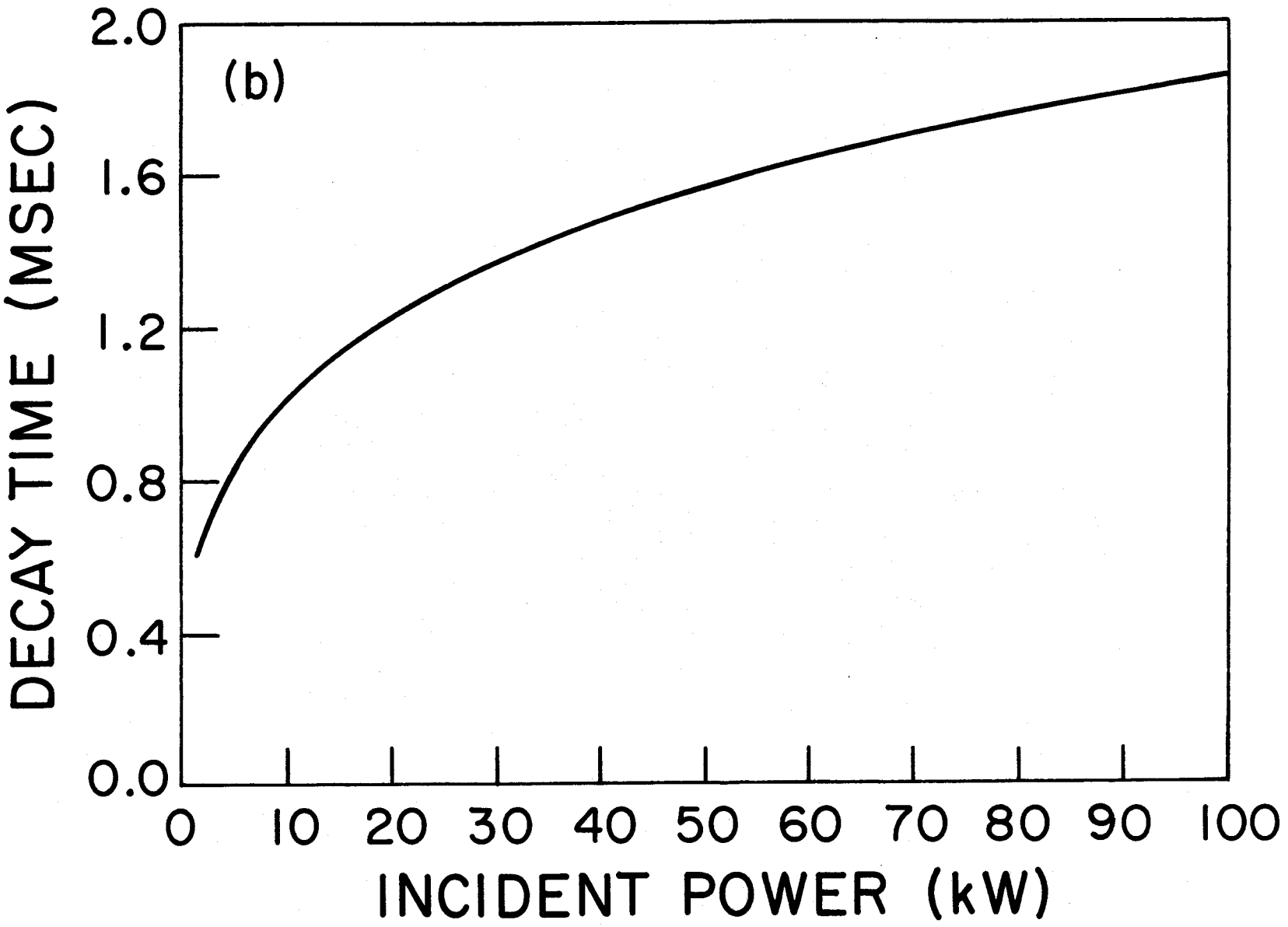
(b)
DECAY TIME (MSEC)
2.0
1.6
1.2
0.8
0.4
0.0
0
10
20
30
40
50
60
70
80
90
100
INCIDENT POWER (kW)

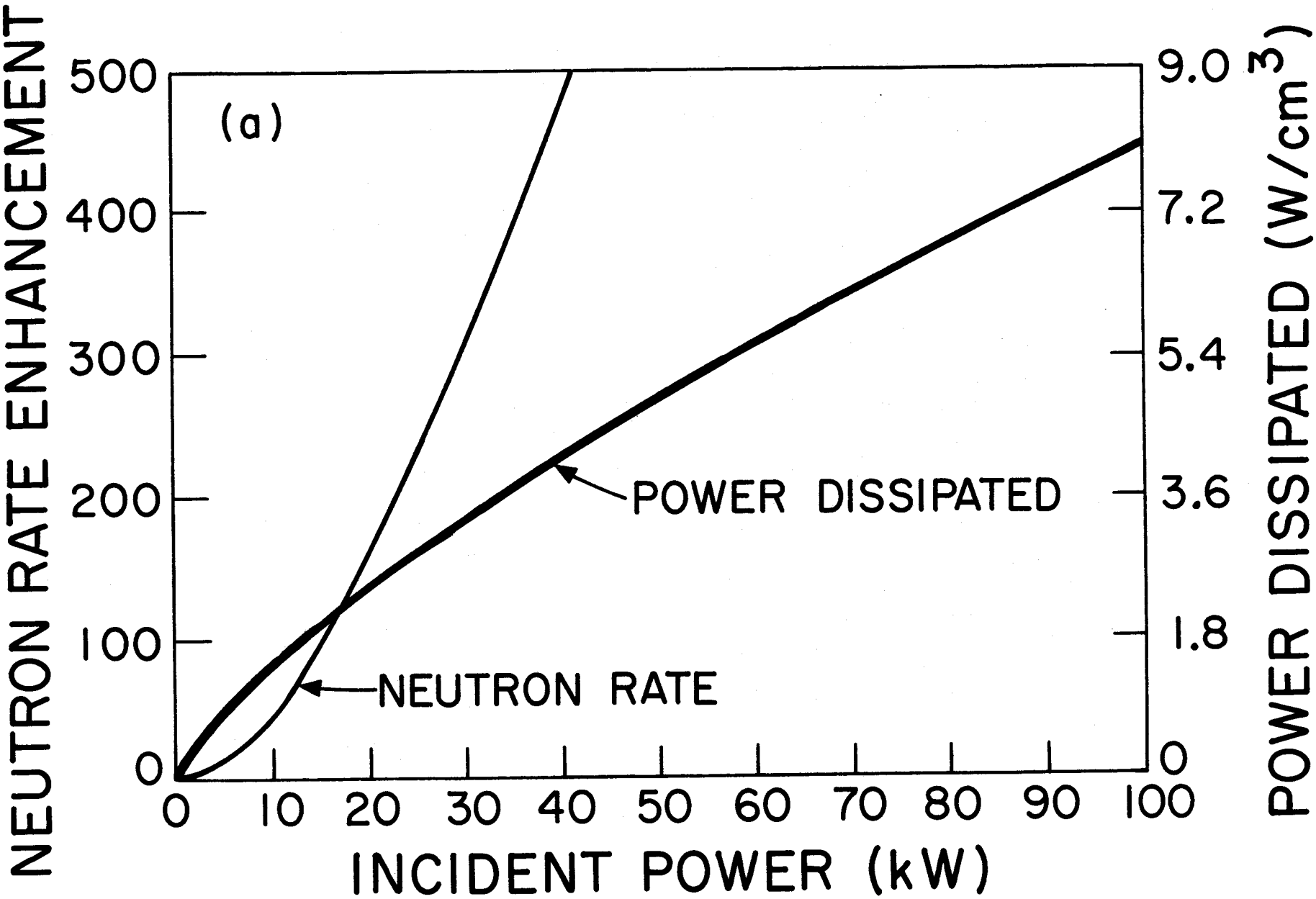
(a)
NEUTRON RATE ENHANCEMENT
500
400
300
200
100
0
POWER DISSIPATED (W/cm^3)
9.0
7.2
5.4
3.6
1.8
0
POWER DISSIPATED
NEUTRON RATE
0
10
20
30
40
50
60
70
80
90
100
INCIDENT POWER (kW)

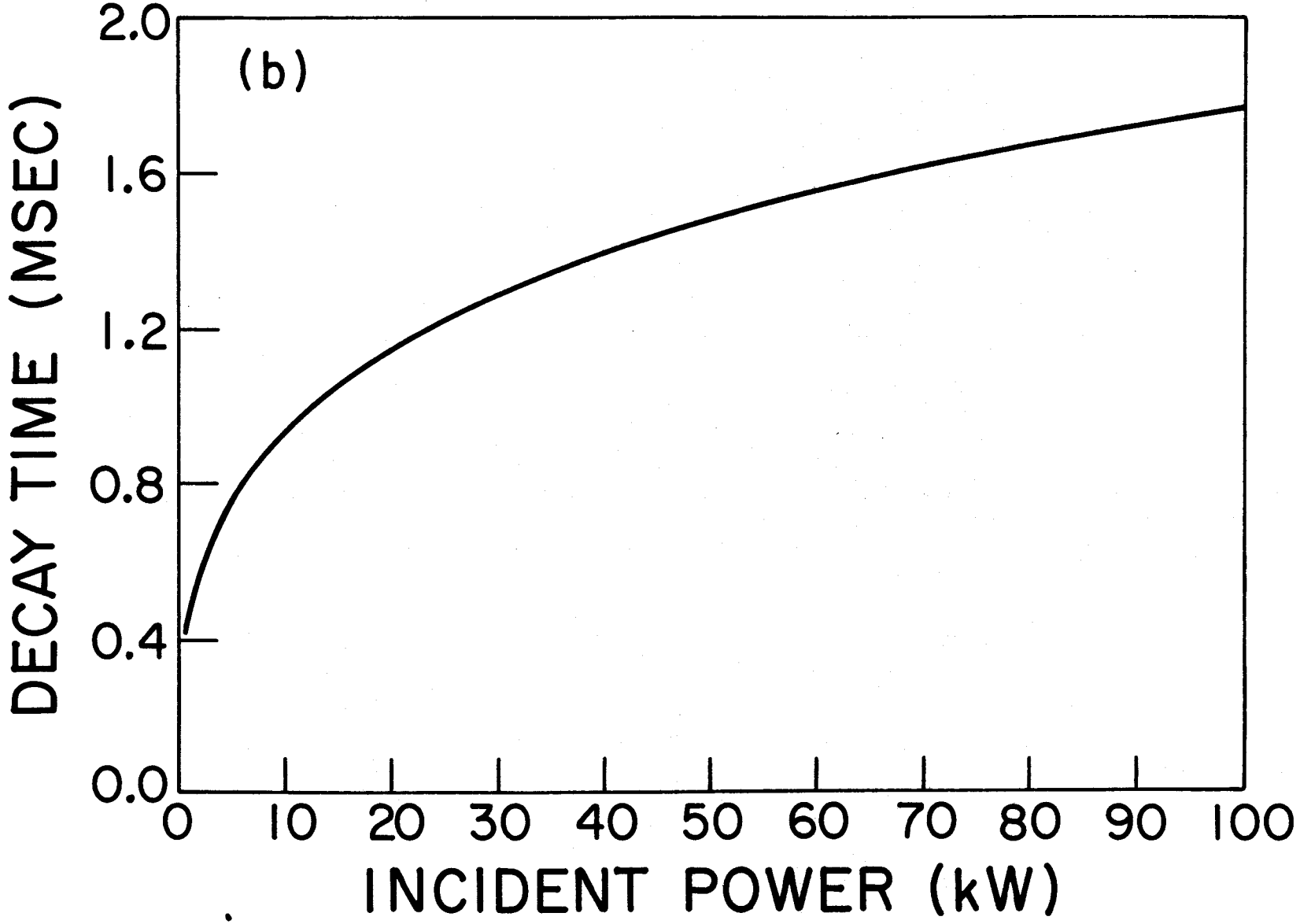
(b)
DECAY TIME (MSEC)
2.0
1.6
1.2
0.8
0.4
0.0
0
10
20
30
40
50
60
70
80
90
100
INCIDENT POWER (kW)

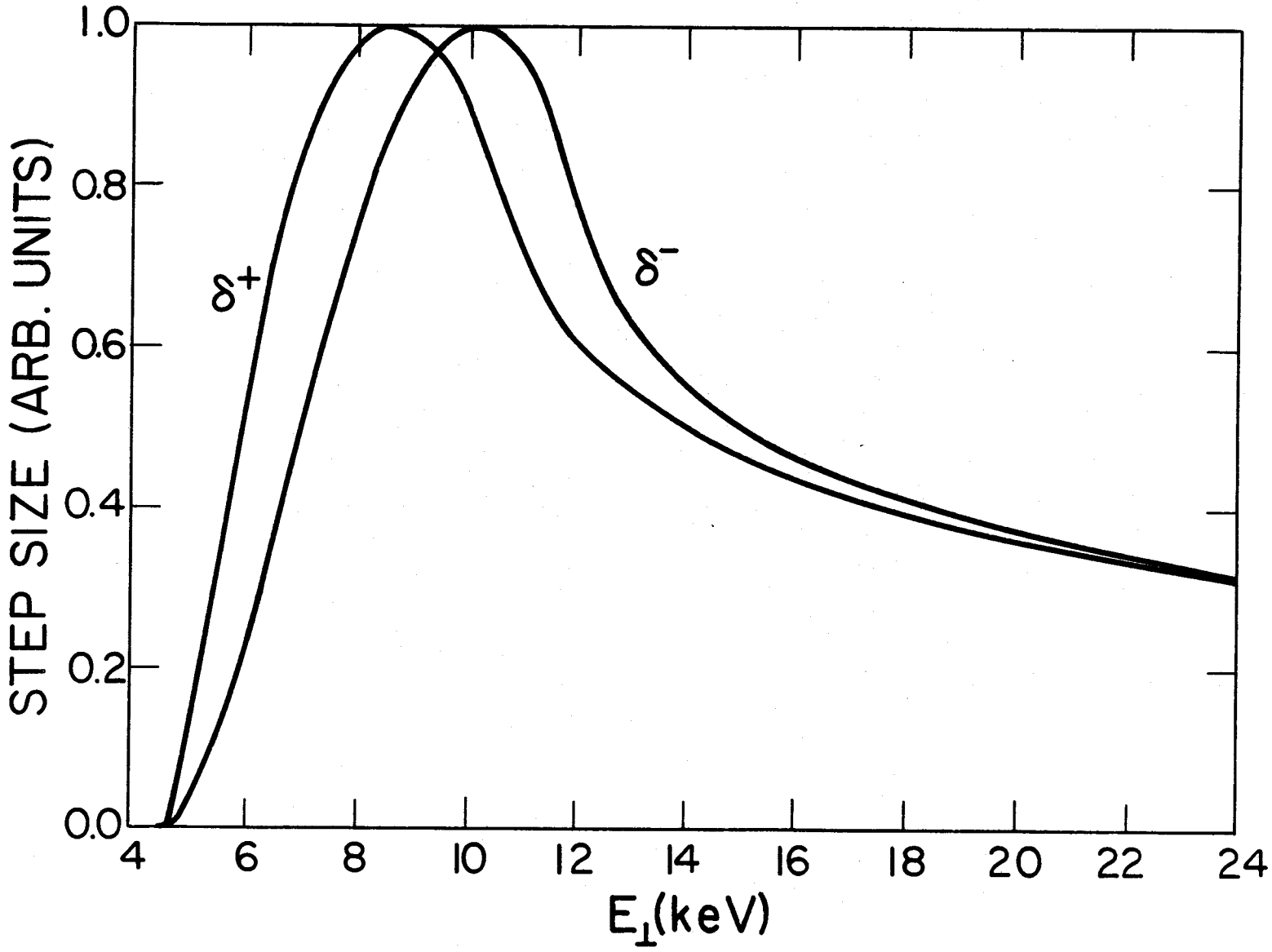
1.0
0.8
0.6
0.4
0.2
0.0
STEP SIZE (ARB. UNITS)
δ+
δ−
4
6
8
10
12
14
16
18
20
22
24
E⊥(keV)

PFC-7016

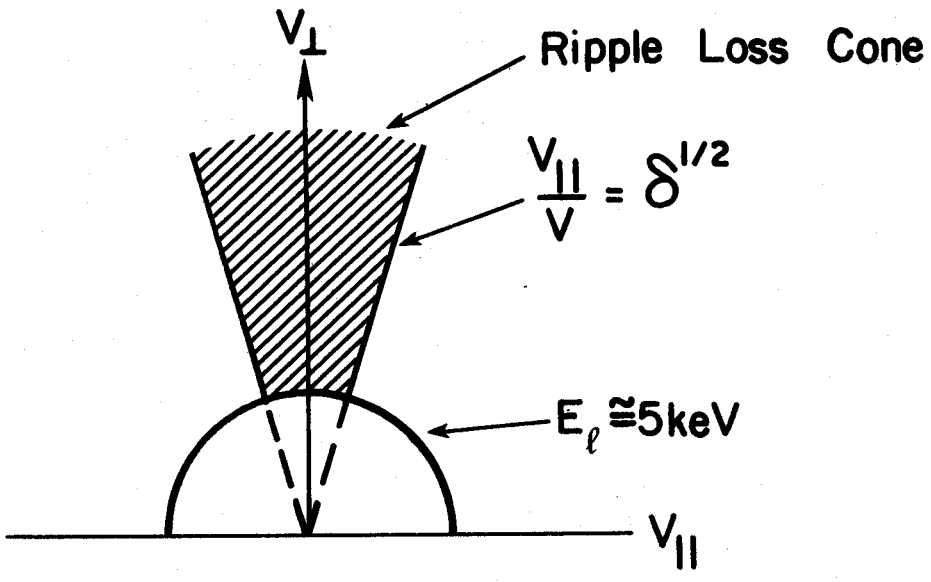

PFC-7013

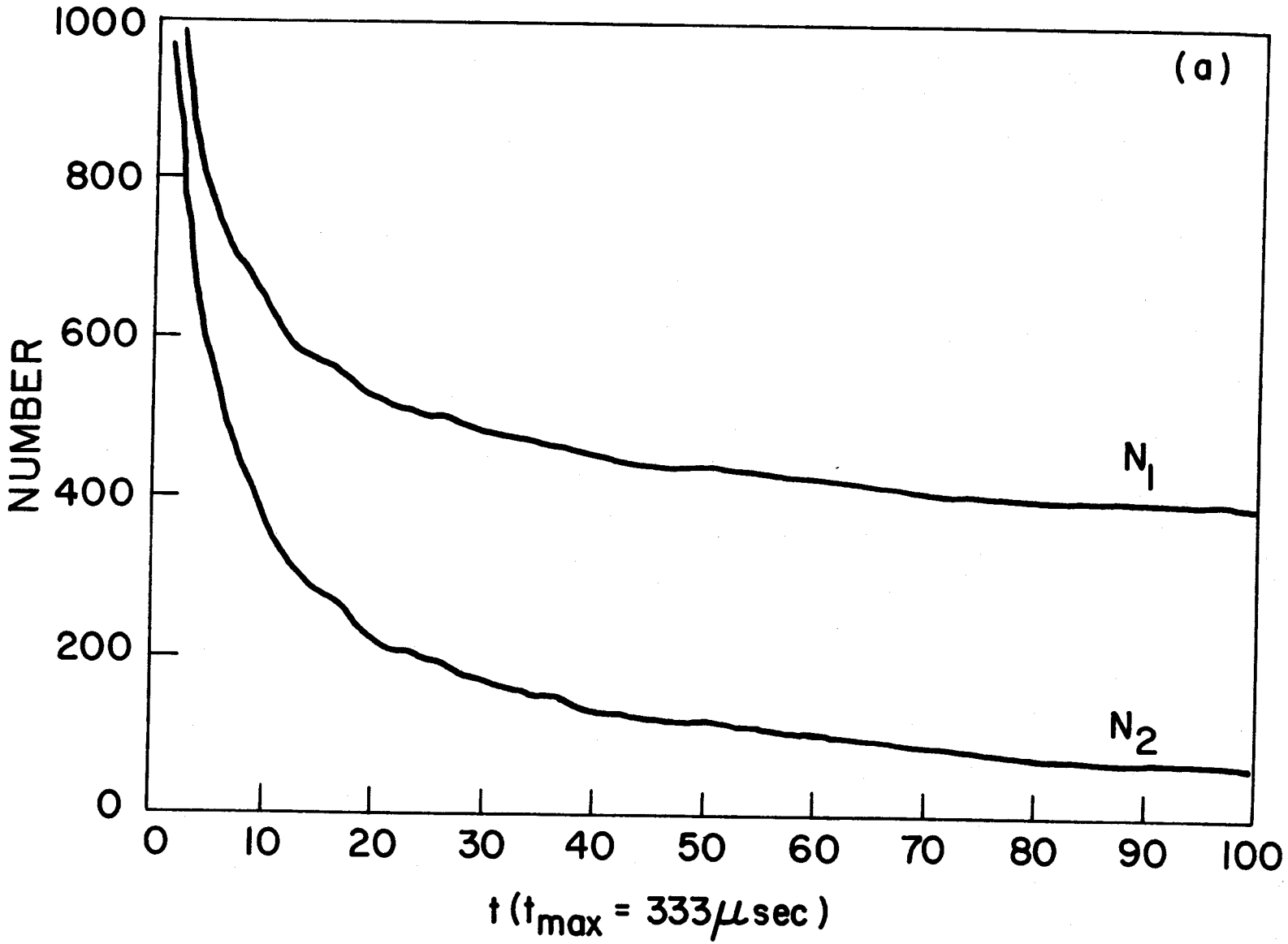
(a)
1000
800
600
400
200
0
NUMBER
N_1
N_2
0
10
20
30
40
50
60
70
80
90
100
t (t_{max} = 333μsec)

PFC-7015

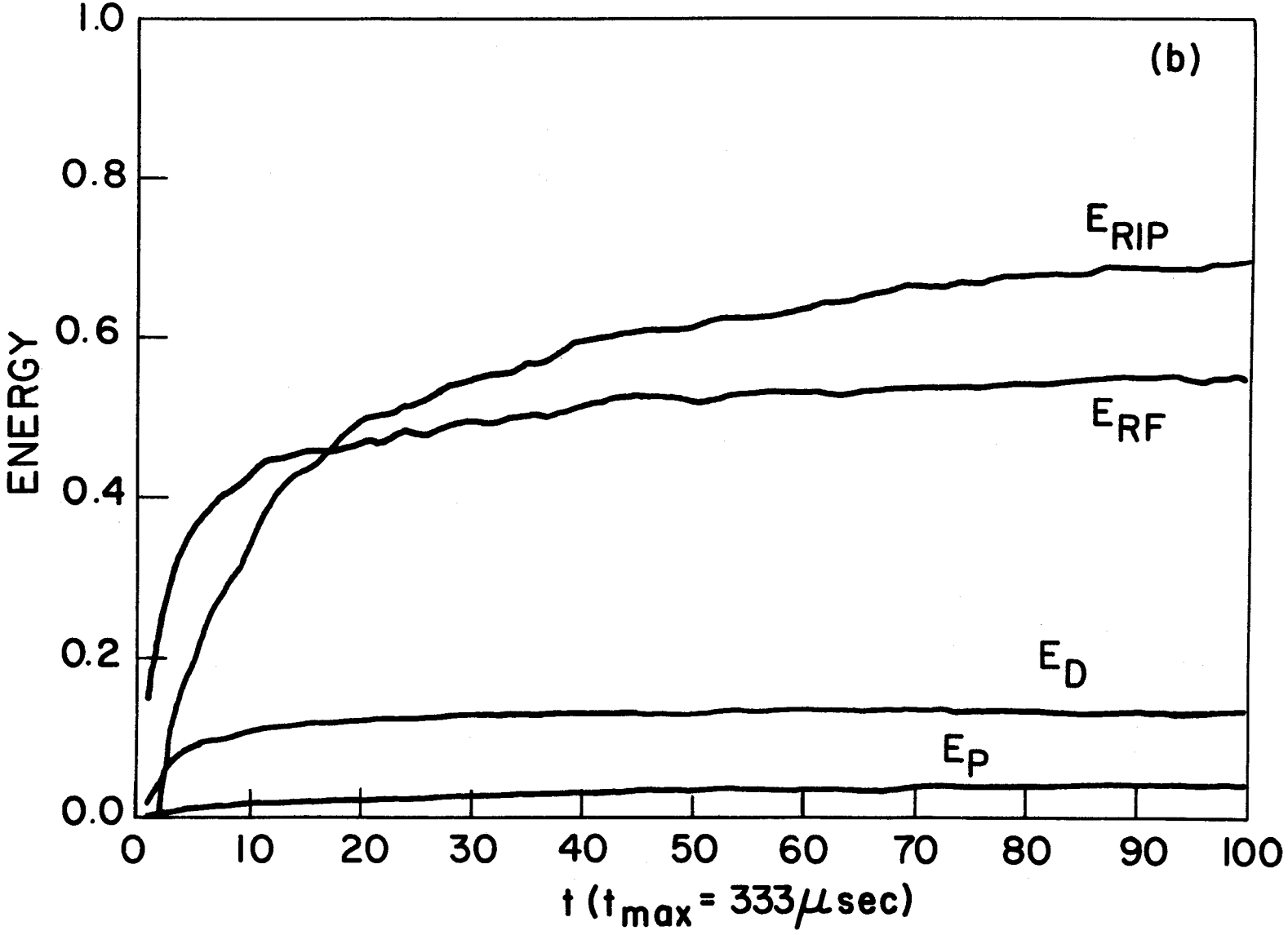
(b)
1.0
0.8
0.6
0.4
0.2
0.0
ENERGY
E_{RIP}
E_{RF}
E_D
E_P
0
10
20
30
40
50
60
70
80
90
100
t (t_{max} = 333μsec)

PFC-7011

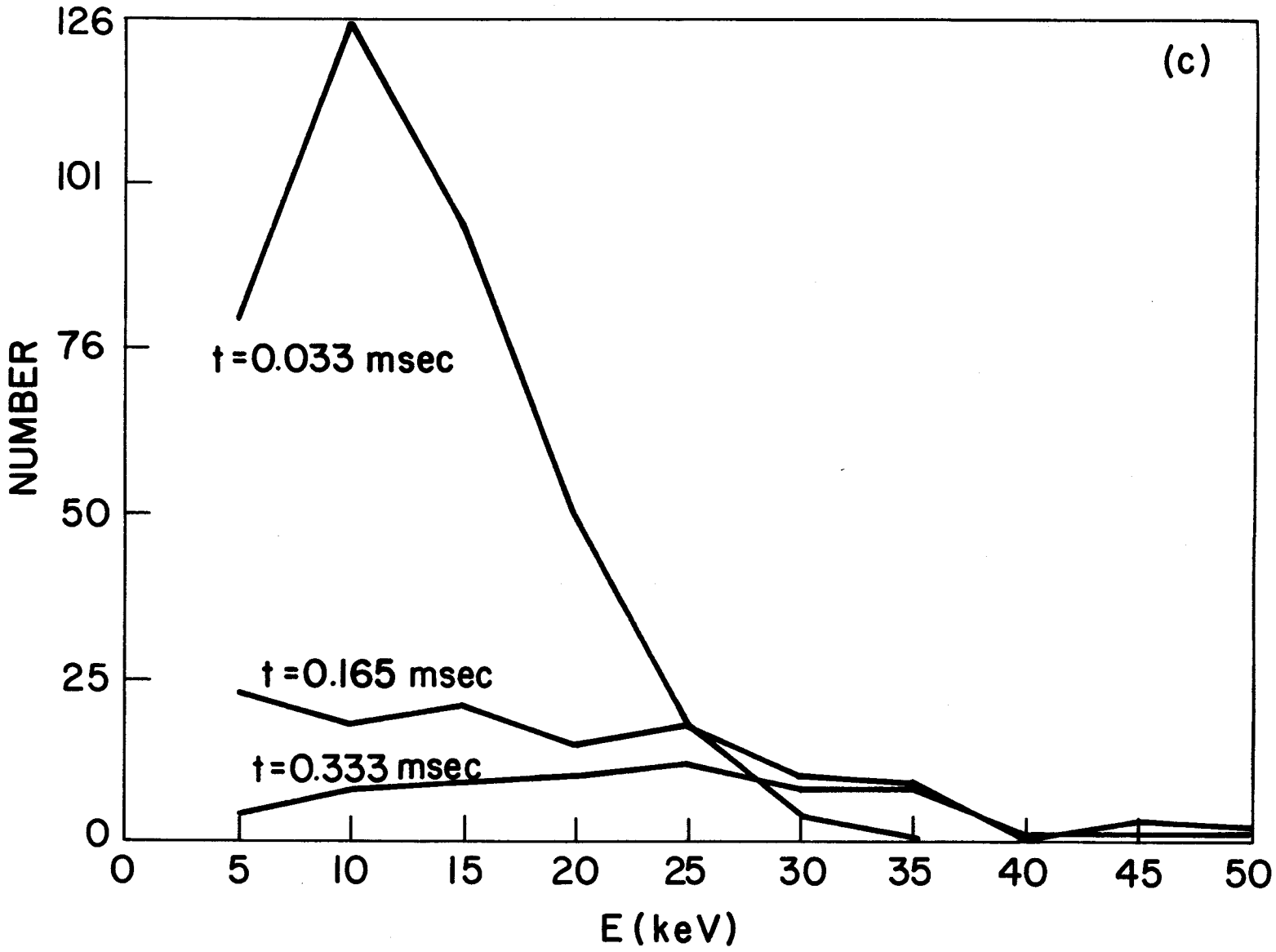
126
101
76
50
25
0
NUMBER
(c)
t=0.033 msec
t=0.165 msec
t=0.333 msec
0
5
10
15
20
25
30
35
40
45
50
E (keV)

PFC-7012

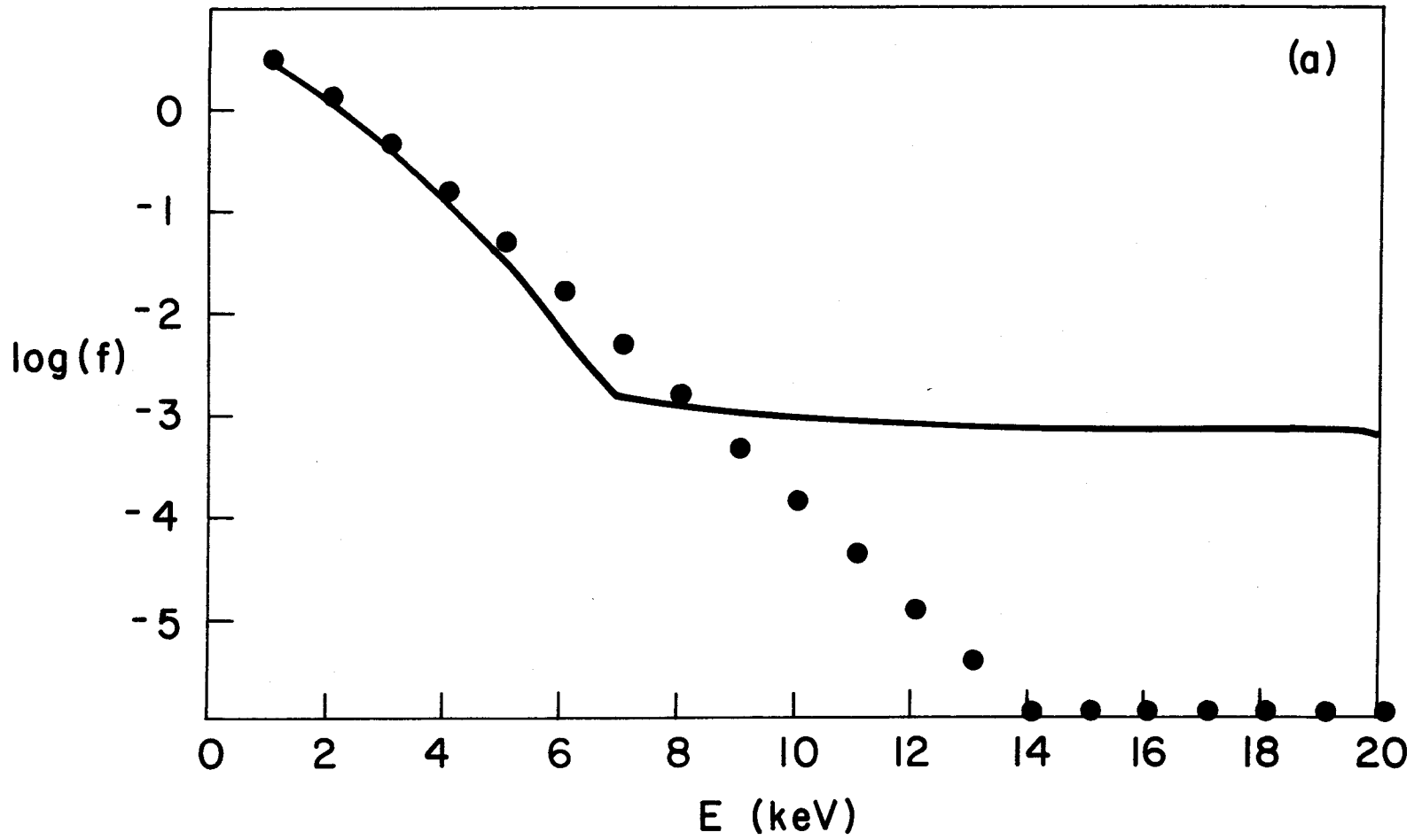
(a)
0
-1
-2
-3
-4
-5
log (f)
0
2
4
6
8
10
12
14
16
18
20
E (keV)
PFC-7017

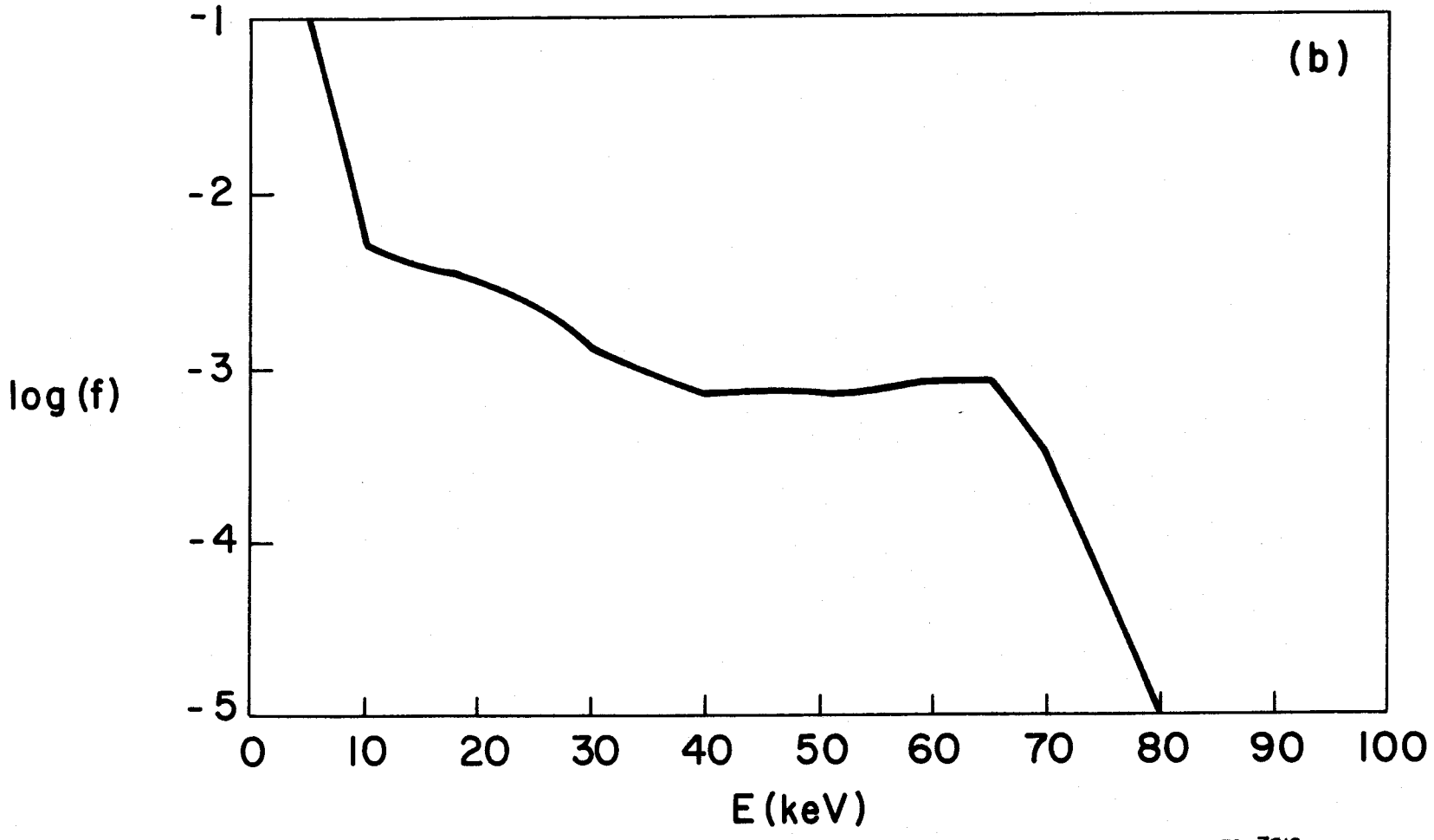
(b)
-1
-2
-3
-4
-5
log (f)
0
10
20
30
40
50
60
70
80
90
100
E (keV)
PFC-7019

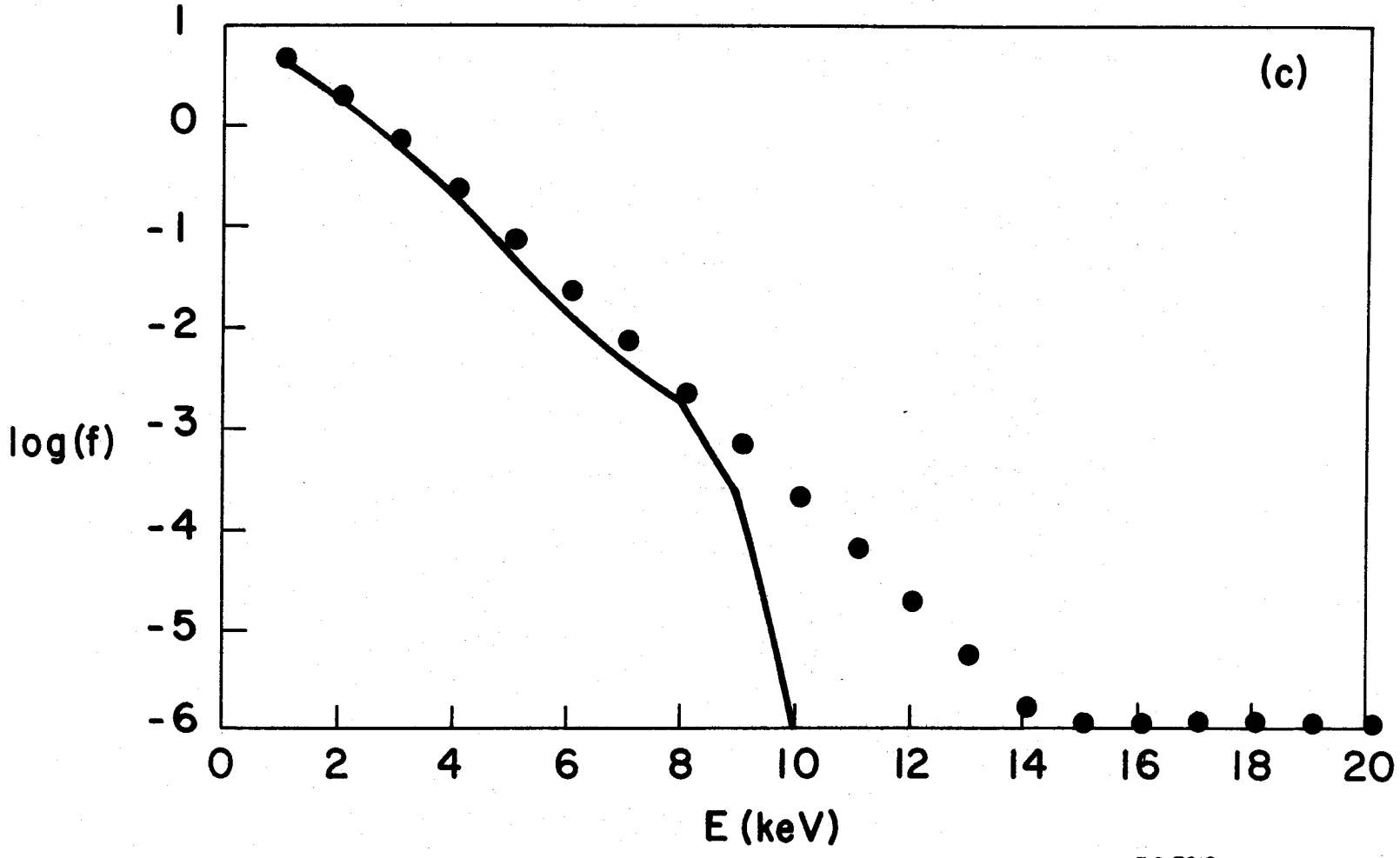
(c)
log(f)
1
0
-1
-2
-3
-4
-5
-6
0
2
4
6
8
10
12
14
16
18
20
E (keV)
PFC-7018